Physics of Riblets

Subjects: Engineering, Aerospace

Contributor: Mohammad Reza Pakatchian , Joana Rocha , Lucy Li

Continuous evolution in nature has created optimum solutions for creature survival that have inspired many innovative engineering designs. Riblet geometries, passive flow control devices, have been studied, which were inspired by the skin of fast-swimming sharks. Turbulent boundary layer research reveals the positive effect of riblets in reducing drag by manipulating turbulent structures.

riblet design turbulent boundary layer drag and noise reduction aircraft

1. Introduction

From billions of years ago until now, continuous evolution in nature has provided high-performance, innovative solutions for the survival of creatures. During the history of science, different research studies have been conducted by imitating nature to make improvements in engineering decisions. The imitation of birds in realizing the long-held dream of humankind for flight is a well-known example of this argument. The emergence of flight was not a conventional replication of the structure of bird wings in detail but was imitated from other naturally evolved methods of birds flying. As an example, there are differences in methods for short- or long-range flying birds [1][2][3][4][5]. As nature has its own solutions for adapting to the environment, in today's eco-friendly optimum engineering designs, imitating these naturally evolved and "optimum solutions" would potentially accelerate technology development and reduce engineering research costs [2][3][5][6].

On this basis, one of the researchers' greatest challenges is finding the cause-and-effect relationship in nature to benefit from natural phenomena in the design of optimized devices. This would be more challenging when optimum results by nature are extracted after a multi-objective evolution, which is improved based on the creature's habitat for different natural reasons [7]. The theory of silent flight is an example investigated by researchers to mimic the noise reduction abilities of owls' wings [8][9][10][11][12][13]. Reducing far-field noise is an important parameter that evolved over the body and wing structure of this species. It is revealed that having large wings with low aspect ratios, serrations in the leading and trailing position of the wings, wavelet-like surfaces, and grooves over the feathers on lower parts of the wings would have a positive effect on reducing radiated noise. The optimum design of shark skin that has contact with water is another example that has evolved by nature. As a multi-objective evolutionary process, the anti-fouling and hydrophobic ability also evolved besides its reduction in drag. The idea of using shark skin structure on the surface that is in contact with the fluid flow is introduced as a solution to reduce frictional drag [14][15][16][17][18]. In this regard, many innovative surfaces replicated from shark skin made their way to the industry, facilitating improvements in engineering designs, especially in friction drag [19].

In aerodynamics, drag is a directional force that acts against movements between fluid and solid body. It always resists movements by producing two main types of resisting forces, named form drag, also known as pressure drag and skin friction drag. Form drag is the opposite force generated by air molecules when flowing past the solid body and pushing it harder against forward rather than backward motion [20]. Skin friction drag, or viscous drag, is the resisting force generated through the moving of fluid flow over the object's surface. Flow viscosity and velocity are the main factors that act on the value of skin friction drag. In addition to the above-mentioned fluid property factors, roughness and surface area exposed to the flow would affect the friction drag value.

Riblets can be considered bio-inspired replications of fast-swimming sharks that acceptably mitigate friction or viscous drag through the surface [14][15][21][22]. These aligned to the flow micro-size geometries can potentially lift high energetic, turbulent vortices from the surface to the riblet tips, leading to less interaction between the surface and turbulent vortices, hence resulting in friction drag reduction [2][23][24][25][26]. Since riblet performance shows the possibility of drag reduction, several numerical and experimental activities have been conducted to investigate different sizes and configurations over these geometries. There is also a wide range of analyses, including simple extrusions as well as complex 3D geometries, combined with various other methods for reducing drag [26][27][28][29][30].

Moreover, riblets show promise for adaptation to various flow control applications for drag reduction, such as aviation, marine ships, automotive, wind energy, sports, and medical fields [1][2][3][17][31][32][33]. Since the first fundamental studies on riblets by the NASA Langley Research Centre in the 1970s [34], many studies have been conducted that show immense potential for drag reduction and greenhouse reduction by sharkskin-inspired riblets in aviation [18][29][35][36][37][38][39][40]. Szodurch estimated that riblets could lead to a 2% draft reduction by an Airbus 320 if 70% of the aircraft is covered with riblets. In 1987, the racing yacht "Stars and Stripes" with the implementation of riblets from NASA and 3M won the America's Cup and the gold medal at Olympia [41]. In 2010, the BMW Oracle team won the 33rd America's Cup with their racing yacht covered with riblets [42], In 2012, riblets found their applications on wind turbine blades [31] and a Formula 1 car by Bionic Surface technology [43]. Moreover, riblets' antifouling properties have been studied for potential applications on marine ships, medical implants, water treatment systems, and food and beverage industries [44][45][46].

Despite the common underlying physics of riblets in drag reduction and other applications, translating riblet technology to different domains poses challenges related to scale, environmental conditions, and surface materials. As an example, in the field of wind energy, wind turbine blades require considerations of larger scales and dynamic load variations, while underwater vehicles involve hydrodynamic complexities. Ensuring the robustness and durability of riblet structures in diverse conditions, as well as addressing manufacturing and maintenance aspects, are key challenges when applying riblet technology [14].

2. Physics of Riblets

Multiple research studies have been undertaken to examine the effectiveness of various riblet geometries in reducing drag. The effectiveness of drag reduction is closely linked to the flow properties, size and configuration of

riblets [23][26][30][47][48]. Some conventional shapes of riblet geometries are illustrated in **Figure 1.** Bladed [47], triangular [29], semi-circular [26][49], trapezoidal [50][51][52][53] and spaced triangular [54] are some of the most conventional geometries. Riblets drag reduction can be characterized by non-dimensional parameters, namely: (1) non-dimensional spacing, defined as $s^+ = s \cdot u\tau / \nu$, in which ν is the kinematic viscosity and $u\tau$ is the friction velocity known as a function of viscous shear stress ($u_\tau = \sqrt{\tau_0 / \rho}$), and (2) non-dimensional height of the grooves (h^+). The non-dimensional parameters are generally used to compare the outcomes of using riblets with available numerical and experimental studies [6][22][51][55]. In addition, by utilizing experimental data from diverse riblet configurations, the square root of non-dimensional riblet cross-section area ($l_g^+ = \sqrt{A_g^+}$) has been introduced [56]. The goal was to determine if it could be feasible to represent drag reduction through a geometric parameter capable of encompassing the combined impact of riblet spacing and shape. This approach was implemented as another effective parameter for the characterization of riblets [57][58].

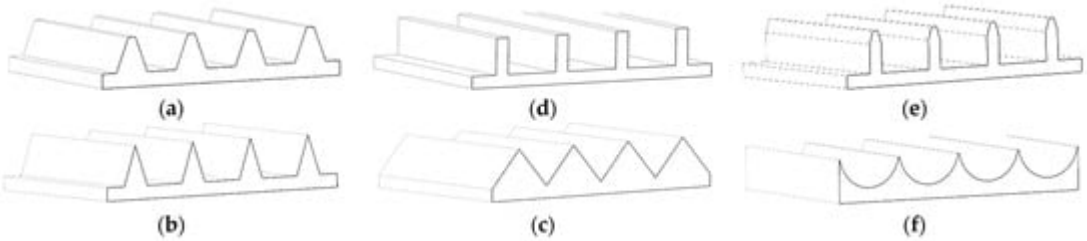

Figure 1. Conventional riblet geometries: (**a**) trapezoidal, (**b**) spaced triangular, (**c**) triangular, (**d**) bladed, (**e**) trapezoidal bladed, and (**f**) semi-circular.

Several researchers have dedicated their studies to investigating the effects of riblets on both boundary layers and free stream flows. Specifically, they have focused on examining the coherent structures present within the turbulent boundary layer, particularly in areas influenced by the wall. These coherent structures exhibit unique characteristics, including smaller sizes and complex three-dimensional fluctuations, which differ from the overall flow behavior [59]. These property fluctuations in the airflow over the surface of a commercial aircraft at an altitude of 12.2 km, with a Mach number (M) of 0.8 and a Reynolds number (Re) of 10^6 can be in the order of microns [32][55].

The coherent structures are a part of the process of sweep and ejection with momentum exchange inside the turbulent boundary layer [18][26][60]. Momentum exchange in the turbulent boundary layer would be accrued by approaching high-speed flows to the surface (known as sweep) that is associated with positive u-component and negative v-component velocities and moving the low-speed flows from the near wall to toward freestream flow (known as ejection) that is associated with negative u-component and positive v-component velocities; this would result in shear stress effects inside the turbulent boundary layer [18][61]. The process of sweep and ejection causes near-wall longitudinal vortices, which lead to small spanwise motions in the viscous sub-layer and then increased friction drag [61]. Riblets, like small longitudinal fences, can hamper the movements of these vortices in such a way as to control skin friction drag [32][35][62][63][64].

Research studies have been mainly focused on the viscous sublayer, the area with y^+<5, given that 50% of turbulent energy is generated in the lower region (i.e., the lower 5% area) of the turbulent boundary layer [65]. To prevent the occurrence of sweep and injection between flow layers, riblet geometries with sizes comparable to the viscous sublayer are necessary. This size requirement ensures effective impedance of the flow interactions and promotes desired flow behavior [21]. A classical definition of drag reduction by riblet surfaces is defined by using the concept of surface-wetted area [21][66]. Compensation of the surface wetted area is an important factor in evaluating the drag reduction performance by riblets. In this context, the level of interaction between surface and fluid flow is an indication of the shear stress and friction drag [17]. In the riblet surfaces, turbulent flow is lifted up and interacts with riblet tips that decrease wetted area and fluid shear stress [67]. In comparison to the smooth surface, adjusting the flow vortices above the valleys of riblets results in lower values of cross-stream flow fluctuations and reduces turbulent kinetic energy near the surface [51][67][68]. Importantly, these adjustments also minimize pressure fluctuations in the outer layers of the flow. These alterations have the potential to influence the emitted sound in compressible fluids, especially in aviation-related contexts [50][51].

As the reduction in wetted area is the main concept behind drag reduction, the number of indentations per unit of length should be within an optimum range [21]. The effect of non-dimensional spacing, s+, in drag reduction for a triangular riblet geometry with peak sharpness of 60° is illustrated in **Figure 2**. The figure indicates the limit of drag reduction when riblets spacing tends to be zero. Drag reduction achieves its optimum values at about s+≈15. Increasing s+ further would result in decreased effectiveness, causing an increase in drag more than zero, which is defined in the figure as a rough surface [35].

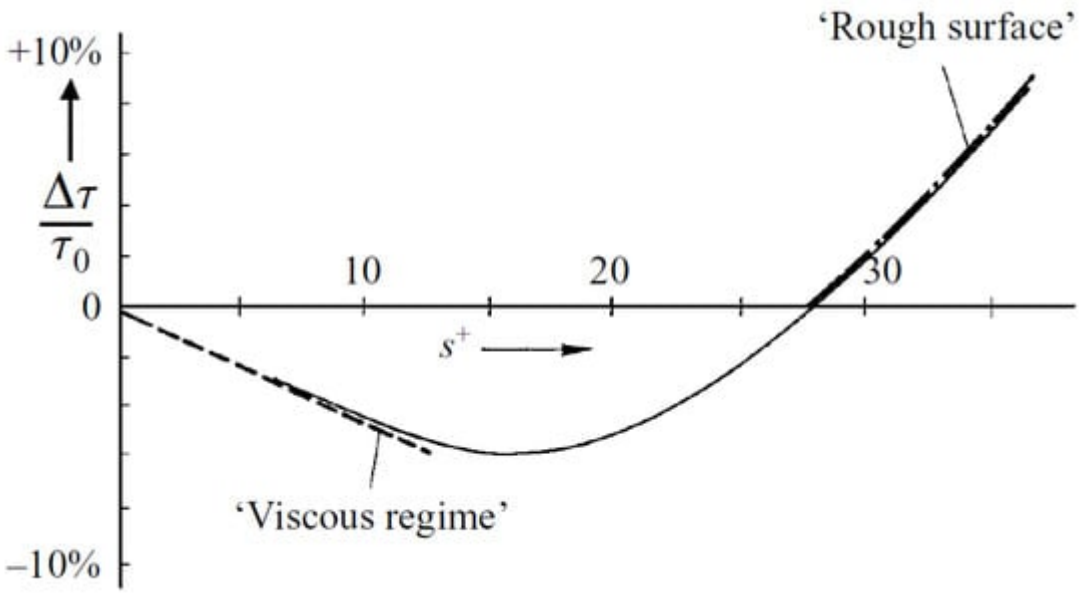

Figure 2. Effect of non-dimensional spacing in a drag reduction of a triangular riblet with 60° peak sharpness [69].

Research efforts have been dedicated to examining the aerodynamic implications of riblets on curved surfaces, particularly in the context of aircraft aerodynamics. Investigations have specifically targeted 3D applications to account for the complexities arising from variations in flow alignment experienced when airflow interacts with

curved surfaces. To address these challenges, researchers have introduced curved riblet configurations featuring diverse riblet shapes, non-dimensional spacing and height. These design considerations aim to optimize drag reduction performance and effectively manage the intricate aerodynamic characteristics associated with curved surfaces [70].

Experimental and numerical studies have been conducted to investigate the impact of riblets on the structure of the boundary layer. To comprehensively understand riblet performance across different scales, a hierarchical analysis approach can be adopted. Starting at the micro-scale, detailed simulations and experiments delve into the fluid dynamics within individual riblet grooves and their interaction with the boundary layer, unveiling insights into local drag reduction mechanisms. Advancing to macro-scale, full-scale computational fluid dynamics simulations can evaluate the overall aerodynamic effect of riblets on complete aircraft systems, considering intricate flow interactions. In the experimental and numerical investigations, both viewpoints are considered separately or in a combined method. Generally speaking, these studies analyze the characteristics of the boundary layer before and after the application of riblets on flat and curved surfaces. The flow properties, including mean and fluctuating terms in the longitudinal, lateral, and vertical directions, are examined. The fluctuating terms not only influence the aerodynamic aspects but also have significant implications for the acoustical properties and generated noise [47][50].

Acknowledging the intersection of experimental and numerical research in exploring the impact of riblets on boundary layer structure, a comprehensive understanding of riblets' performance across diverse scales can be achieved through a hierarchical analysis framework. This approach entails a progression from the micro-scale, where detailed simulations and experiments illustrate the fluid dynamics within individual riblet grooves and their interaction with the boundary layer, showing localized drag reduction mechanisms. Advancing to the macro-scale, extensive computational fluid dynamics simulations assess the aerodynamic influence of riblets on aircraft systems, encompassing intricate flow interactions. Broadly, these inquiries dissect the characteristics of the boundary layer in both pre and post-riblet application on both flat and curved surfaces. Flow properties, including mean and fluctuating components along the longitudinal, lateral, and vertical axes, undergo meticulous examination. Significantly, these fluctuating terms extend their influence beyond aerodynamics, affecting acoustical attributes and noise generation [47][50].

References

1. Hwang, J.; Jeong, Y.; Park, J.M.; Lee, K.H.; Hong, J.W.; Choi, J. Biomimetics: Forecasting the Future of Science, Engineering, and Medicine. Int. J. Nanomed. 2015, 10, 5701.
2. Bhushan, B. Biomimetics: Lessons from Naturean Overview. Philos. Trans. R. Soc. A Math. Phys. Eng. Sci. 2009, 367, 1445–1486.
3. Bhushan, B. Biomimetics. Philos. Trans. R. Soc. A Math. Phys. Eng. Sci. 2009, 367, 1443–1444.

4. Zhang, Y.; Meng, W.; Fan, B.; Tang, W. Biomimetic Optimization Research on Wind Noise Reduction of an Asymmetric Cross-Section Bar. Springerplus 2016, 5, 1221.
5. Jung, Y.C.; Bhushan, B. Biomimetic Structures for Fluid Drag Reduction in Laminar and Turbulent Flows. J. Phys. Condens. Matter 2010, 22, 035104.
6. Bechert, D.W.; Bruse, M.; Hage, W.; Meyer, R. Fluid Mechanics of Biological Surfaces and Their Technological Application. Naturwissenschaften 2000, 87, 157–171.
7. Jo, S.; Ahn, S.; Lee, H.; Jung, C.-M.; Song, S.; Kim, D.R. Water-Repellent Hybrid Nanowire and Micro-Scale Denticle Structures on Flexible Substrates of Effective Air Retention. Sci. Rep. 2018, 8, 16631.
8. Jiakun, H.; Zhe, H.; Fangbao, T.; Gang, C. Review on Bio-Inspired Flight Systems and Bionic Aerodynamics. Chin. J. Aeronaut. 2021, 34, 170–186.
9. Weger, H.; Weger, M.; Klaas, M.; Schröder, W. Features of Owl Wings That Promote Silent Flight. Interface Focus 2017, 7, 78.
10. Jaworski, J.W.; Peake, N. Aeroacoustics of Silent Owl Flight. Annu. Rev. Fluid Mech. 2020, 52, 395–420.
11. Clark, C.J.; Lepiane, K.; Liu, L. Evolution and Ecology of Silent Flight in Owls and Other Flying Vertebrates. Integr. Org. Biol. 2020, 2, obaa001.
12. Sagar, P.; Teotia, P.; Sahlot, A.D.; Thakur, H.C. An Analysis of Silent Flight of Owl. Mater. Today Proc. 2017, 4, 8571–8575.
13. Wang, Y.; Zhao, K.; Lu, X.Y.; Song, Y.B.; Bennett, G.J. Bio-Inspired Aerodynamic Noise Control: A Bibliographic Review. Appl. Sci. 2019, 9, 2224.
14. Dean, B.; Bhushan, B. Shark-Skin Surfaces for Fluid-Drag Reduction in Turbulent Flow: A Review. Philos. Trans. R. Soc. A Math. Phys. Eng. Sci. 2010, 368, 4775–4806.
15. Bechert, D.W.; Hoppe, G.; Reif, W.E. On the Drag Reduction of the Shark Skin. In Proceedings of the 23rd Aerospace Sciences Meeting, Reno, NV, USA, 14–17 January 1985.
16. Bechert, D.W.; Bartenwerfer, M.; Hoppe, G.; Reif, W.-E. Drag Reduction Mechanisms Derived from Shark Skin. AIAA 1986, 2, 1044–1068.
17. Fu, Y.F.; Yuan, C.Q.; Bai, X.Q. Marine Drag Reduction of Shark Skin Inspired Riblet Surfaces. Biosurf. Biotribol. 2017, 3, 11–24.
18. Bechert, D.W.; Hage, W. Drag Reduction with Riblets in Nature and Engineering. In Flow Phenomena in Nature; WIT Press: Southampton, UK, 2006; Volume 2, pp. 457–504.
19. Nature as a Role Model: Lufthansa Group and BASF Roll Out Sharkskin Technology. Available online: https://www.basf.com/global/en/media/news-releases/2021/05/p-21-204.html (accessed on

3 May 2021).

20. Brostow, W. Drag Reduction in Flow: Review of Applications, Mechanism and Prediction. J. Ind. Eng. Chem. 2008, 14, 409–416.
21. Martin, S.; Bhushan, B. Modeling and Optimization of Shark-Inspired Riblet Geometries for Low Drag Applications. J. Colloid. Interface Sci. 2016, 474, 206–215.
22. Bixler, G.D.; Bhushan, B. Shark Skin Inspired Low-Drag Microstructured Surfaces in Closed Channel Flow. J. Colloid. Interface Sci. 2013, 393, 384–396.
23. WALSH, M. Turbulent Boundary Layer Drag Reduction Using Riblets. In Proceedings of the 20th Aerospace Science Meeting, Orlando, FL, USA, 11–14 January 1982.
24. Bhushan, B. Nanotribology and Nanomechanics: An Introduction, 4th ed.; Springer: Berlin/Heidelberg, Germany, 2017; pp. 1–928.
25. Choi, K.S. Smart Flow Control with Riblets. Adv. Mat. Res. 2013, 745, 27–40.
26. Walsh, M.J.; Lindemann, A.M. Optimization and Application of Riblets for Turbulent Drag Reduction. In Proceedings of the 22nd Aerospace Sciences Meeting, Reno, NV, USA, 9–12 January 1984.
27. Xu, F.; Zhong, S.; Zhang, S. Vortical Structures and Development of Laminar Flow over Convergent-Divergent Riblets. Phys. Fluids 2018, 30, 051901.
28. Guo, T.; Zhong, S.; Craft, T. Secondary Flow in a Laminar Boundary Layer Developing over Convergent-Divergent Riblets. Int. J. Heat Fluid Flow 2020, 84, 108598.
29. Walsh, M. Drag Characteristics of V-Groove and Transverse Curvature Riblets. In Viscous Flow Drag Reduction; American Institute of Aeronautics and Astronautics, Inc.: Reston, VA, USA, 1980; pp. 168–184.
30. Bechert, D.W.; Bruse, M.; Hage, W. Experiments with Three-Dimensional Riblets as an Idealized Model of Shark Skin. Exp. Fluids 2000, 28, 403–412.
31. Sareen, A.; Deters, R.W.; Henry, S.P.; Selig, M.S. Drag Reduction Using Riblet Film Applied to Airfoils for Wind Turbines. J. Sol. Energy Eng. Trans. ASME 2014, 136, 021007.
32. Martin, S.; Bhushan, B. Fluid Flow Analysis of Continuous and Segmented Riblet Structures. RSC Adv. 2016, 6, 10962–10978.
33. Wen, L.; Weaver, J.C.; Lauder, G.V. Biomimetic Shark Skin: Design, Fabrication and Hydrodynamic Function. J. Exp. Biol. 2014, 217, 1656–1666.
34. WALSH, M.; WEINSTEIN, L. Drag and Heat Transfer on Surfaces with Small Longitudinal Fins. In Proceedings of the 11th Fluid and PlasmaDynamics Conference, Seattle, WA, USA, 10–12 July 1978.

35. Bechert, D.W.; Bruse, M.; Hage, W.; Van Der Hoeven, J.G.T.; Hoppe, G. Experiments on Drag-Reducing Surfaces and Their Optimization with an Adjustable Geometry. J. Fluid Mech. 1997, 338, 59–87.
36. Ciliberti, D.; Della Vecchia, P.; Memmolo, V.; Nicolosi, F.; Wortmann, G.; Ricci, F. The Enabling Technologies for a Quasi-Zero Emissions Commuter Aircraft. Aerospace 2022, 9, 319.
37. Cacciatori, L.; Brignoli, C.; Mele, B.; Gattere, F.; Monti, C.; Quadrio, M. Drag Reduction by Riblets on a Commercial UAV. Appl. Sci. 2022, 12, 5070.
38. Ran, W.; Zare, A.; Jovanović, M.R. Model-Based Design of Riblets for Turbulent Drag Reduction. J. Fluid Mech. 2021, 906, A7.
39. Endrikat, S.; Modesti, D.; García-Mayoral, R.; Hutchins, N.; Chung, D. Influence of Riblet Shapes on the Occurrence of Kelvin-Helmholtz Rollers. J. Fluid Mech. 2021, 913, A37.
40. Zhang, Z.L.; Zhang, M.M.; Cai, C.; Cheng, Y. Characteristics of Large- and Small-Scale Structures in the Turbulent Boundary Layer over a Drag-Reducing Riblet Surface. Proc. Inst. Mech. Eng. C J. Mech. Eng. Sci. 2020, 234, 796–807.
41. NASA—NASA Riblets for Stars & Stripes. Available online: https://www.nasa.gov/centers/langley/news/factsheets/Riblets.html (accessed on 19 July 2021).
42. BMW ORACLE Racing Wins 33rd America’s Cup. The US-Challenger Defeats the Defender 2 to 0. Available online: https://www.press.bmwgroup.com/global/article/detail/T0077733EN/bmw-oracle-racing-wins-33rd-america%E2%80%99s-cup-the-us-challenger-defeats-the-defender-2-to-0?language=en (accessed on 14 September 2023).
43. Riblets Competence—Bionic Surface Technologies. Available online: https://www.bionicsurface.com/riblets-competence/ (accessed on 14 September 2023).
44. Chen, D.; Liu, Y.; Chen, H.; Zhang, D. Bio-inspired Drag Reduction Surface from Sharkskin. Biosurf. Biotribol. 2018, 4, 39–45.
45. Bilinsky, H.C.; Builth-Williams, J.; Quinn, M. Curing Functional Properties into UV Coatings: Direct Contactless Microfabrication of Drag Reducing, Anti-Bacterial, Anti-Fouling and Optical Microstructures. In Proceedings of the adTech NA Conference, Milano, Italy, 27–28 May 2020.
46. Zhang, D.; Chen, H.; Jiang, Y.; Cai, J.; Feng, L.; Zhang, X. Bionic Drag Reduction Surface from Shark Skin and Bioinspired Anti-Icing Surface from Superhydrophobic Lotus Leaf. Micro-Nano-Bionic Surf. 2022, 2022, 197–226.
47. Choi, K. so Near-Wall Structure of a Turbulent Boundary Layer with Riblets. J. Fluid Mech. 1989, 208, 417–458.
48. Sundaram, S.; Viswanath, P.R.; Rudrakumar, S. Viscous Drag Reduction Using Riblets on NACA 0012 Airfoil to Moderate Incidence. AIAA J. 1996, 34, 676–682.

49. Saravi, S.S.; Cheng, K. A review of drag reduction by riblets and micro-textures in the turbulent boundary layers. Eur. Sci. J. ESJ 2013, 9, 62–81.
50. Muhammad, C.; Chong, T.P. Mitigation of Turbulent Noise Sources by Riblets. J. Sound Vib. 2022, 541, 117302.
51. Choi, K.S. The Wall-Pressure Fluctuations of Modified Turbulent Boundary Layer with Riblets; International Union of Theoretical and Applied Mechanics; Springer: Berlin/Heidelberg, Germany, 1988.
52. Stenzel, V.; Wilke, Y.; Hage, W. Drag-Reducing Paints for the Reduction of Fuel Consumption in Aviation and Shipping. Prog. Org. Coat. 2011, 70, 224–229.
53. Grüneberger, R.; Hage, W. Drag Characteristics of Longitudinal and Transverse Riblets at Low Dimensionless Spacings. Exp. Fluids 2011, 50, 363–373.
54. Suzuki, Y.; Kasagi, N. Turbulent Drag Reduction Mechanism above a Riblet Surface. AIAA J. 1994, 32, 1781–1790.
55. Walsh, M.J. Riblets as a Viscous Drag Reduction Technique. AIAA J. 1983, 21, 485–486.
56. García-Mayoral, R.; Jiménez, J. Hydrodynamic Stability and Breakdown of the Viscous Regime over Riblets. J. Fluid Mech. 2011, 678, 317–347.
57. Mele, B. Riblet Drag Reduction Modeling and Simulation. Fluids 2022, 7, 249.
58. Mele, B.; Tognaccini, R.; Catalano, P. Performance Assessment of a Transonic Wing–Body Configuration with Riblets Installed. J. Aircr. 2016, 53, 129–140.
59. Robinson, S.K. The Kinematics of Turbulent Boundary Layer Structure. NASA Technical Memorandum; NASA Ames Research Center: Moffett Field, CA, USA, 1991.
60. Choi, K.S. A Survey of the Turbulent Drag Reduction Using Passive Devices. STIN 1984, 85, 20268.
61. Karniadakis, G.E.; Choi, K.-S. Mechanisms On Transverse Motions In Turbulent Wall Flows. Annu. Rev. Fluid Mech. 2003, 35, 45–62.
62. Hage, W.; Bechert, D.W.; Bruse, M. Yaw Angle Effects on Optimized Riblets. In Aerodynamic Drag Reduction Technologies; Springer: Berlin/Heidelberg, Germany, 2001; pp. 278–285.
63. Rastegari, A.; Akhavan, R. The Common Mechanism of Turbulent Skin-Friction Drag Reduction with Superhydrophobic Longitudinal Microgrooves and Riblets. JFM 2018, 838, 68–104.
64. Walsh, M.J.; Sellers, W.L.; McGinley, C.B. Riblet Drag at Flight Conditions. J. Aircr. 1988, 26, 570–575.
65. Bushnell, D.M.; Hefner, J.N. Viscous Drag Reduction in Boundary Layers; American Institute of Aeronautics and Astronautics: Washington, DC, USA, 1990; ISBN 978-0-930403-66-9.

66. Choi, H.; Moin, P.; Kim, J. Direct Numerical Simulation of Turbulent Flow over Riblets. J. Fluid Mech. 1993, 255, 503–539.
67. Chu, D.; Karniadakis, G.E. A Direct Numerical Simulation of Laminar and Turbulent Flow over Riblet-Mounted Surfaces. J. Fluid Mech. 1993, 250, 1–42.
68. Park, S.R.; Wallace, J.M. Flow Alteration and Drag Reduction by Riblets in a Turbulent Boundary Layer. AIAA J. 1994, 32, 31–38.
69. Nieuwstadt, F.T.M.; Wolthers, W.; Leijdens, H.; Krishna Prasad, K.; Schwarz-van Manen, A. The Reduction of Skin Friction by Riblets under the Influence of an Adverse Pressure Gradient. Exp. Fluids 1993, 15, 17–26.
70. Bilinsky, H.C. Direct Contactless Microfabrication of 3D Riblets: Improved Capability and Metrology. In Proceedings of the AIAA Scitech 2019 Forum, San Diego, CA, USA, 7–11 January 2019.